Supplementary material for the article:

Macháčková, K.; Chrudinová, M.; Radosavljević, J.; Potalitsyn, P.; Křížková, K.; Fábry, M.; Selicharová, I.; Collinsová, M.; Brzozowski, A. M.; Žáková, L.; et al. Converting Insulin-like Growth Factors 1 and 2 into High-Affinity Ligands for Insulin Receptor Isoform A by the Introduction of an Evolutionarily Divergent Mutation. *Biochemistry* **2018**, *57* (16), 2373–2382. https://doi.org/10.1021/acs.biochem.7b01260

Supporting Information

for

Converting Insulin-like Growth Factors 1 and 2 into High-Affinity Ligands for Insulin Receptor Isoform A by the Introduction of an Evolutionarily Divergent Mutation

Kateřina Macháčková, Martina Chrudinová, Jelena Radosavljević, Pavlo Potalitsyn, Květoslava Křížková, Milan Fábry, Irena Selicharová, Michaela Collinsová, Andrzej M. Brzozowski, Lenka Žáková* and Jiří Jiráček*

Table of Contents

Table S1. Mutagenesis strategies used for cloning of successfully expressed and produced IGF-1 and IGF-2 analogs.

Analog (expression construct)	Mutation(s)	Forward mutagenic primer (5′-3′)	Reverse mutagenic primer (5′-3′)	Template construct	Applied strategy
Gly-1-IGF-1	-				
[His45]-IGF-1	[D45H]	CCGGCATTGTGCACGAATGCT GCTTTCGC	GCGAAAGCAGCATTCGTGCA CAATGCCGG	Gly-1-IGF-1	SDM
[Asn45]-IGF-1	[D45N]	CCGGCATTGTTAACGAATGCT GCTTTCGC	GCGAAAGCAGCATTCGTTAA CAATGCCGG	Gly-1-IGF-1	SDM
[Ala45]-IGF-1	[D45A]	CCGGCATTGTGGCGGAATGCT GCTTTCGC	GCGAAAGCAGCATTCCGCCA CAATGCCGG	Gly-1-IGF-1	SDM
[His46]-IGF-1	[E46H]	CCGGCATTGTGGATCACTGCT GCTTTCGC	GCGAAAGCAGCAGTGATCCA CAATGCCGG	Gly-1-IGF-1	SDM
[Gln46]-IGF-1	[E46Q]	CCGGCATTGTGGATCAATGCT GCTTTCGC	GCGAAAGCAGCATTGATCCA CAATGCCGG	Gly-1-IGF-1	SDM
[Ala46]-IGF-1	[E46A]	CCGGCATTGTGGATGCATGCT GCTTTCGC	GCGAAAGCAGCATGCATCCA CAATGCCGG	Gly-1-IGF-1	SDM
[Asn45,Gln46]-IGF-1	[D45N+E46Q]	ACCGGCATTGTTAACCAGTGC TGCTTTCGCAGC	GCTGCGAAAGCAGCACTGGT TAACAATGCCGGT	Asn45-IGF-1	OE
[His49]-IGF-1	[F49H]	GTGGATGAATGCTGCCATCGC AGCTGCGATCTG	CAGATCGCAGCTGCGATGGC AGCATTCATCCAC	Gly-1-IGF-1	OE
His46,His49]-IGF-1	[E46H+F49H]	GTGGATCACTGCTGCCACCGC AGCTGCGATCTG	CAGATCGCAGCTGCGGTGGC AGCAGTGATCCAC	His46-IGF-1	SDM
[Gln46,His49]-IGF-1	[E46Q+F49H]	GTGGATCAATGCTGCCATCGC AGCTGCGATCTG	CAGATCGCAGCTGCGATGGC AGCATTGATCCAC	Gln46-IGF-1	OE
[Asn45,Gln46,His49]-IGF-1	[D45N+E46Q+F49H]	ATTGTTAACCAGTGCTGCCATC GCAGCTGCGATCT	AGATCGCAGCTGCGATGGCA GCACTGGTTAACAAT	Asn45-IGF-1	OE
IGF-2	-				
[Gln45]-IGF-2	[E45Q]	CGCGGCATTGTGGAACAGTGC TGCTTTCGCAGC	GCTGCGAAAGCAGCACTGTT CCACAATGCCGCG	IGF-2	SDM
[His48]-IGF-2	[F48H]	GTGGAAGAATGCTGCCATCGC AGCTGCGATCTG	CAGATCGCAGCTGCGATGGC AGCATTCTTCCAC	IGF-2	OE
[Gln45,His48]-IGF-2	[E45H+F48H]	CGCGGCATTGTGGAACAGTGC TGCCATCGCAGC	GCTGCGATGGCAGCACTGTT CCACAATGCCGCG	His48-IGF-2	SDM

OE - overlap-extension PCR (*1*), SDM - site-directed mutagenesis of the whole plasmid (*2*).

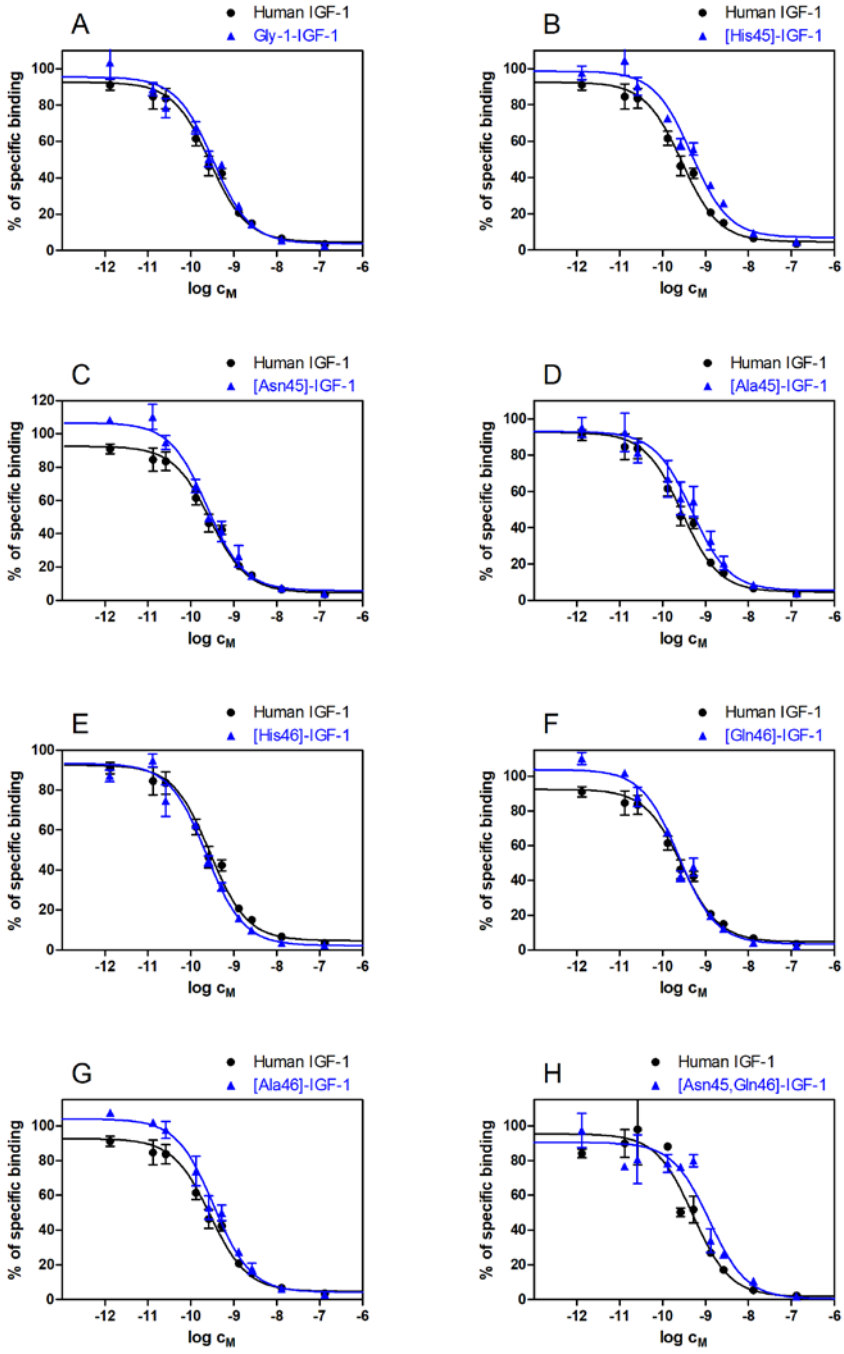

Figure S1. Inhibition of binding of human [^{125}I]monoiodotyrosyl-IGF-1 to human IGF-1R in mouse embryonic fibroblasts by Gly-1-IGF-1 (**A**), [His45]-IGF-1 (**B**), [Asn45]-IGF-1 (**C**), [Ala45]-IGF-1 (**D**), [His46]-IGF-1 (**E**), [Gln46]-IGF-1 (**F**), [Ala46]-IGF-1 (**G**), [Asn45,Gln46]-IGF-1 (**H**) and by human IGF-1 (in all panels). All IGF-1 analogs have Gly at the position -1. The representative binding curves are shown.

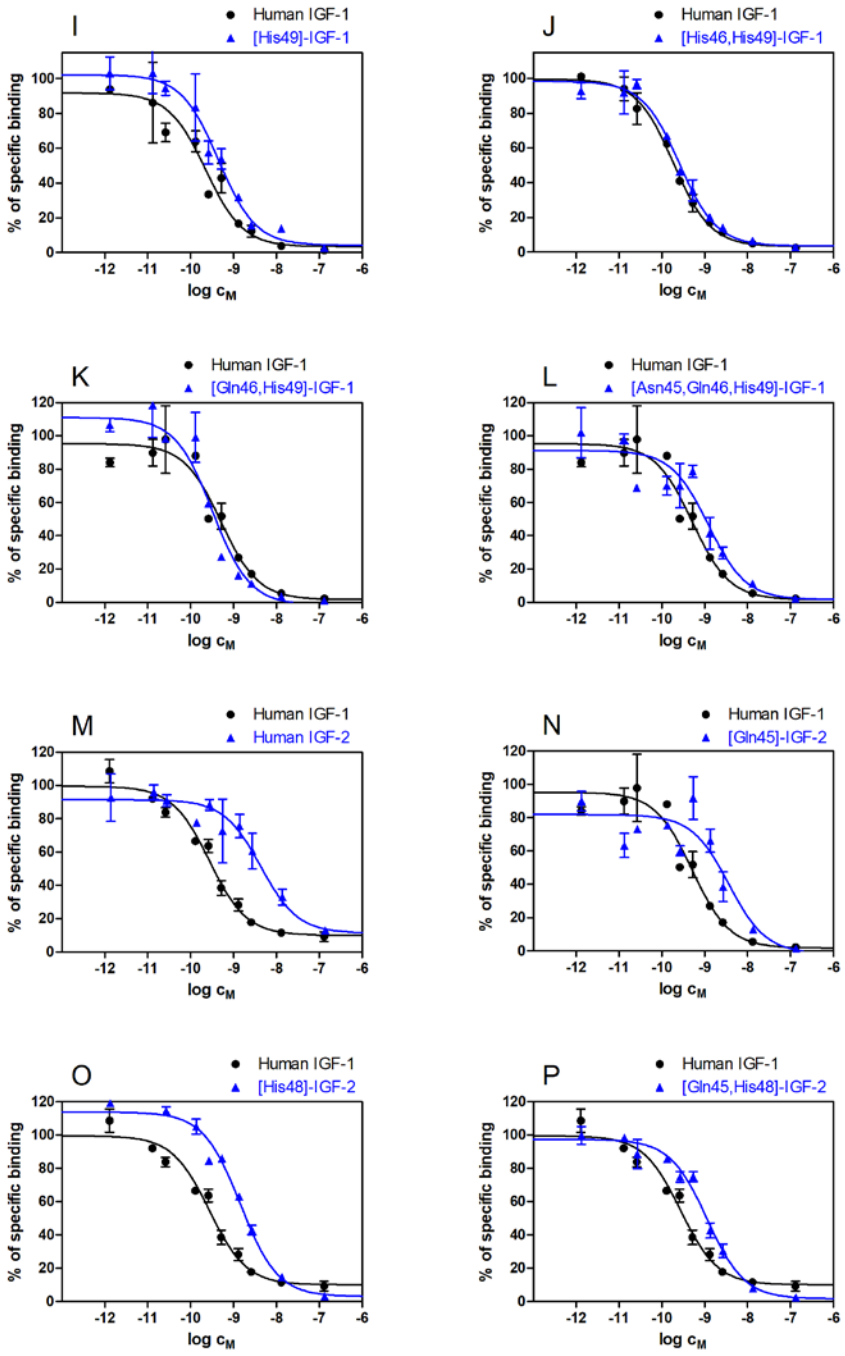

Figure S1 (continued). Inhibition of binding of human [^{125}I]monoiodotyrosyl-IGF-1 to human IGF-1R in mouse embryonic fibroblasts by [His49]-IGF-1 (**I**), [His46,His49]-IGF-1 (**J**), [Gln46,His49]-IGF-1 (**K**), [Asn45,Gln46,His49]-IGF-1 (**L**), human IGF-2 (**M**), [Gln45]-IGF-2 (**N**), [His48]-IGF-2 (**O**), [Gln45,His48]-IGF-2 (**P**) and by human IGF-1 (in all panels). All IGF-1 analogs have Gly at the position -1. The representative binding curves are shown.

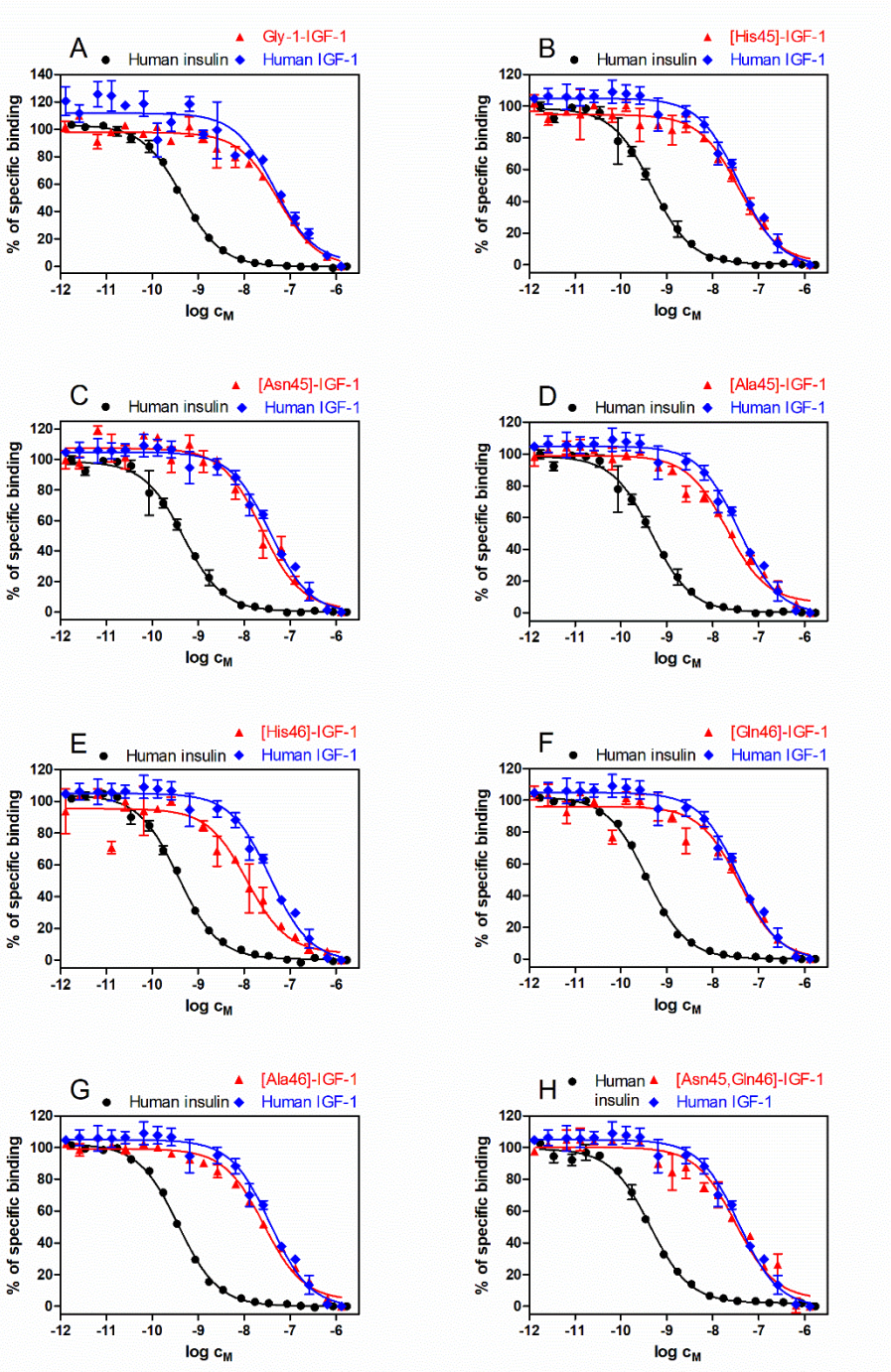

Figure S2. Inhibition of binding of human [^{125}I]monoiodotyrosyl-insulin to human IR-A in human IM-9 lymphocytes by Gly-1-IGF-1 (**A**), [His45]-IGF-1 (**B**), [Asn45]-IGF-1 (**C**), [Ala45]-IGF-1 (**D**), [His46]-IGF-1 (**E**), [Gln46]-IGF-1 (**F**), [Ala46]-IGF-1 (**G**), [Asn45,Gln46]-IGF-1 (**H**) and by human insulin and human IGF-1 (in all panels). All IGF-1 analogs have Gly at the position -1. The representative binding curves are shown.

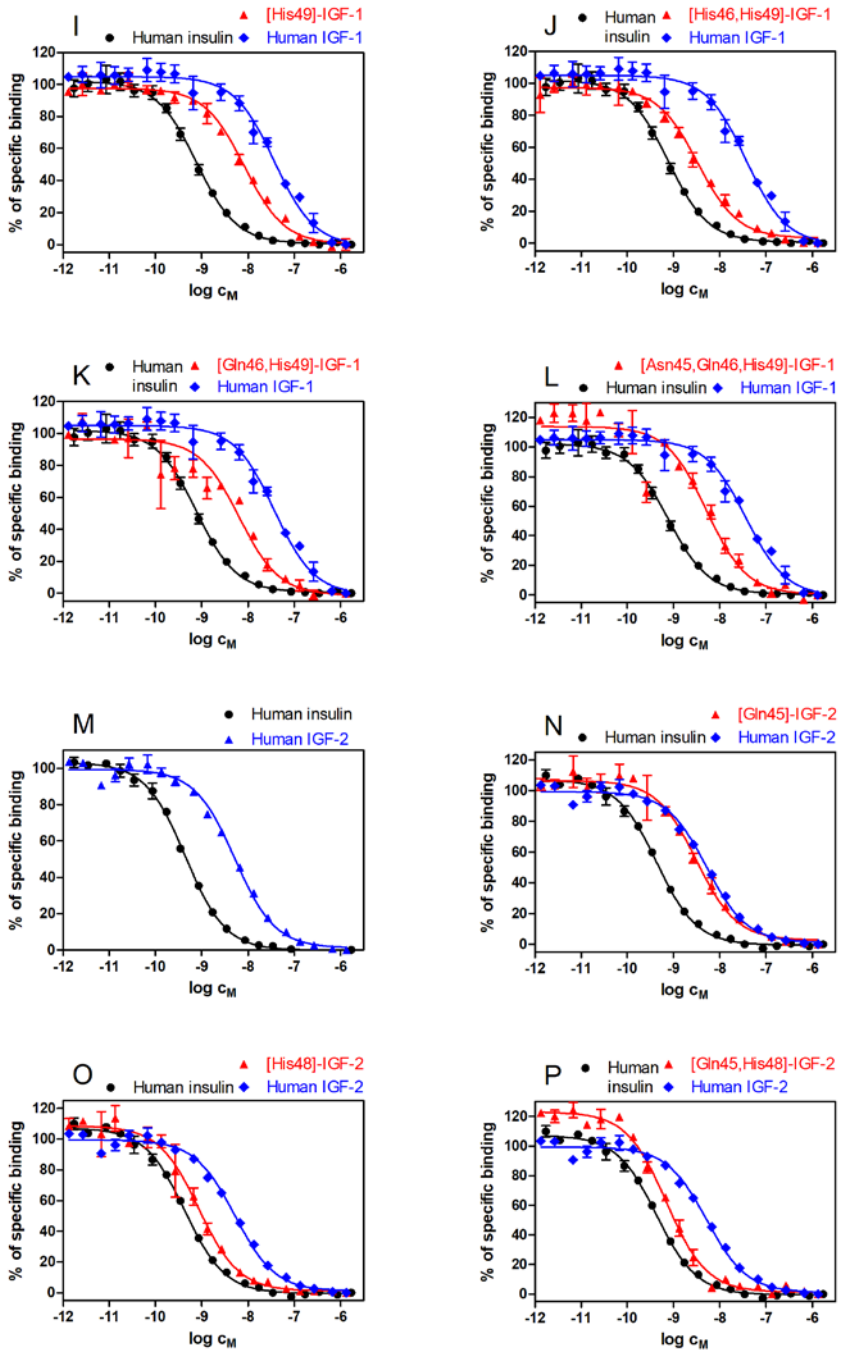

Figure S2 (continued). Inhibition of binding of human [^{125}I]monoiodotyrosyl-insulin to human IR-A in human IM-9 lymphocytes by [His49]-IGF-1 (**I**), [His46,His49]-IGF-1 (**J**), [Gln46,His49]-IGF-1 (**K**), [Asn45,Gln46,His49]-IGF-1 (**L**), human IGF-2 (**M**), [Gln45]-IGF-2 (**N**), [His48]-IGF-2 (**O**), [Gln45,His48]-IGF-2 (**P**) and by human insulin (in all panels), human IGF-1 (in panels **I**-**L**) and human IGF-2 (in panels **M**-**P**). All IGF-1 analogs have Gly at the position -1. The representative binding curves are shown.

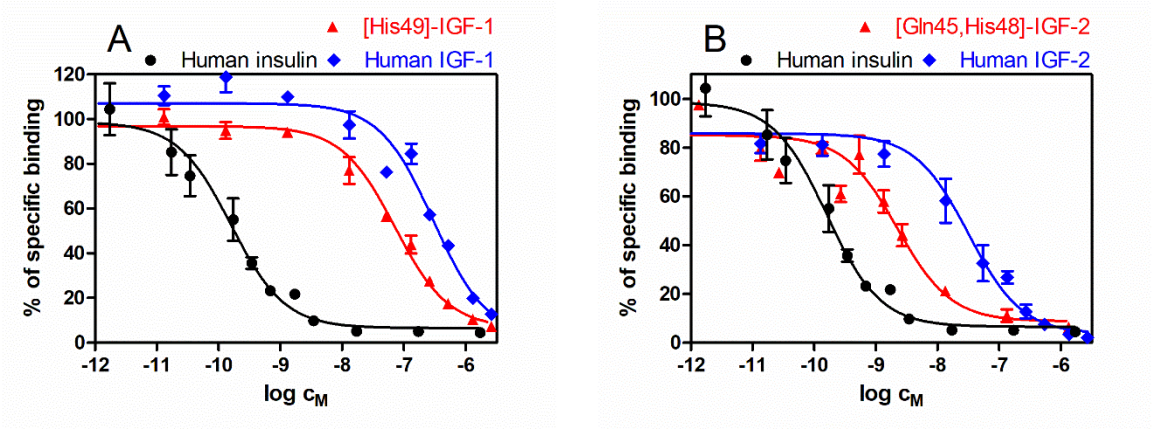

Figure S3. Inhibition of binding of human [^{125}I]monoiodotyrosyl-insulin to human IR-B in mouse embryonic fibroblasts by human insulin, human IGF-1 and by [His49]-IGF-1 (in panel **A**), and by human insulin, human IGF-2 and by [Gln45,His48]-IGF-2 (in panel **B**)**.** The representative binding curves are shown.

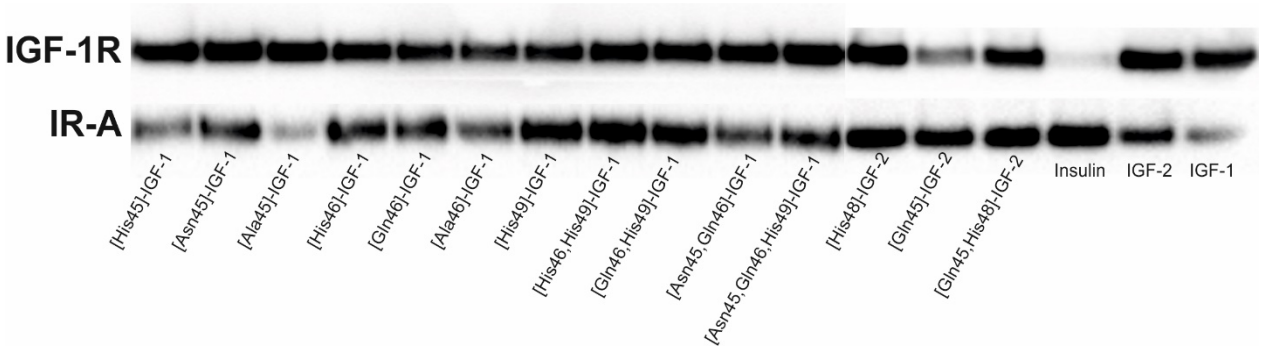

Figure S4. A representative example of immunoblot used for evaluation of abilities of analogs to induce the autophosphorylation of IGF-1R and IR-A at 10 nM concentration of the ligands.

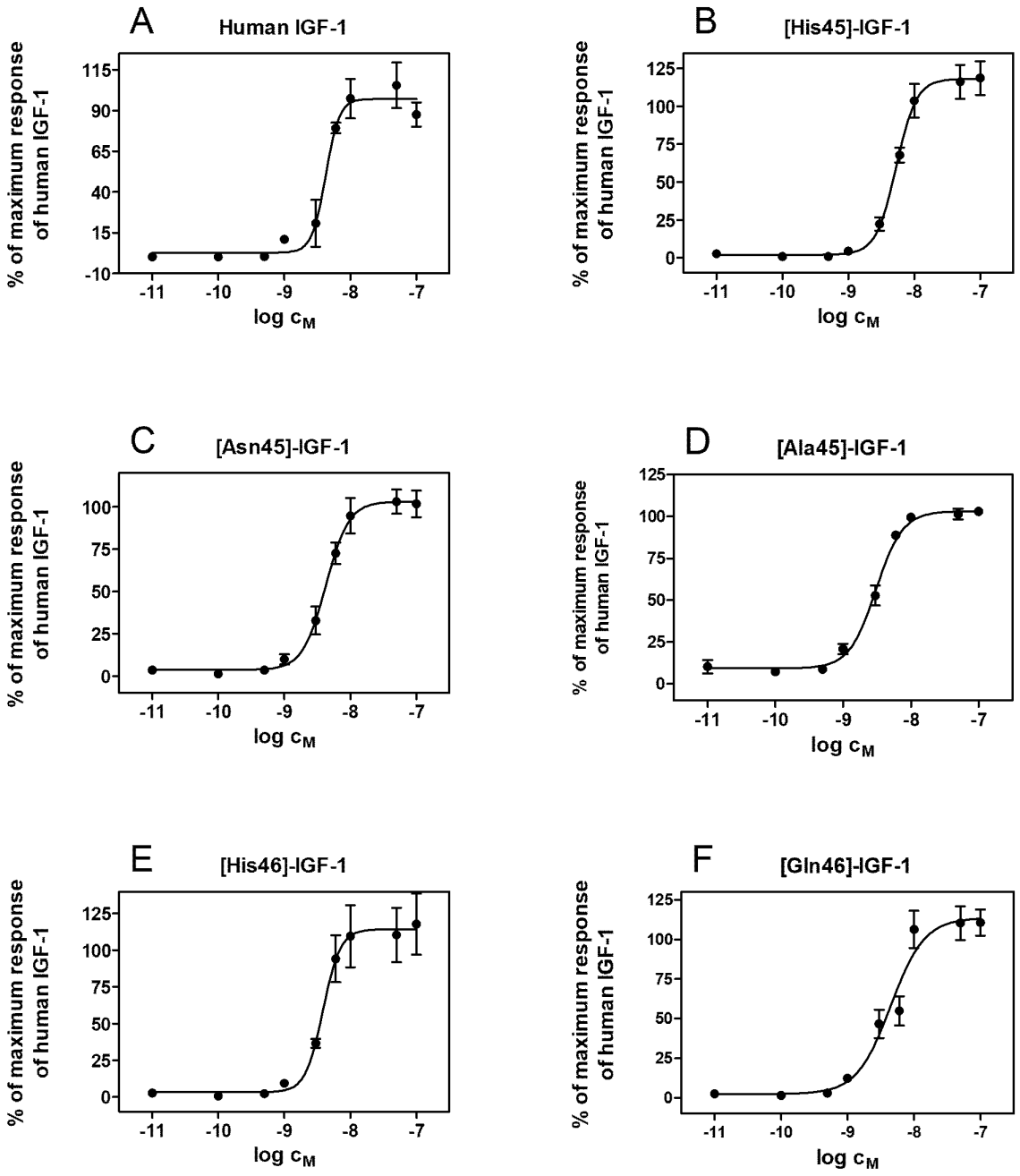

Figure S5. Representative dose response curves of the abilities of human IGF-1 and selected IGF-1 analogs to stimulate autophosphorylation of IGF-1R. Stimulation by human IGF-1 is shown in panel **A**, by [His45]-IGF-1 in panel **B**, by [Asn45]-IGF-1 in panel **C**, by [Ala45]-IGF-1 in panel D, by [His46]-IGF-1 in panel **E** and by [Gln45]-IGF-1 in panel **F**. The EC_{50} values are shown in Table S2.

Table S2. Comparison of abilities of selected IGF-1 analogs to activate IGF-1R in a dose response manner (EC_{50} values) with their ability to activate IGF-1R at 10 nM concentration.

Analog	Ability to activate autophosphorylation of IGF-1R EC_{50} ± S.D. [nM] (n)	Relative ability[a] to activate autophosphorylation of IGF-1R [%]	Relative activation of IGF-1R at 10 nM [%] ± S.D. (n)
human IGF-1	3.7 ± 0.7 (3)	100 ± 19	100 ± 13 (4)
[His45]-IGF-1	5.4 ± 0.5 (3)	69 ± 6	71 ± 20 (4)
[Asn45]-IGF-1	4.7 ± 0.8 (3)	79 ± 13	88 ± 18 (4)
[Ala45]-IGF-1	3.1 ± 0.4 (3)	119 ± 15	80 ± 25 (4)
[His46]-IGF-1	4.4 ± 0.6 (4)	84 ± 11	71 ± 11 (4)
[Gln46]-IGF-1	4.4 ± 1.6 (3)	84 ± 30	69 ± 13 (4)

[a] Relative ability to activate autophosphorylation of the receptor is defined as (EC_{50} of human IGF-1/EC_{50} of analog) x 100.

References:

1. Heckman, K. L., and Pease, L. R. (2007) Gene splicing and mutagenesis by PCR-driven overlap extension, *Nat. Protoc. 2*, 924-932.
2. Laible, M., and Boonrod, K. (2009) Homemade site directed mutagenesis of whole plasmids, *J. Vis. Exp. 27*, e1135, doi:10.3791/1135.